
Mansoura Veterinary Medical Journal

ULTRASTRUCTURE OF THE OLFATORY REGION IN DOGS (CANIS FAMILIARIS) IN RELATION TO HISTOCHEMISTRY & IMMUNO-HISTOCHEMISTRY

Salah EL-Morsi¹, Galal Youssef², Safwat Ebada³, Sahar Ebrahim^{1*}

Department of Anatomy and Embryology, Faculty of Veterinary Medicine, Mansoura University

ABSTRACT

The present study was carried out on clinically healthy and mature five dogs (Canis Familiaris) of both sexes. The tissue specimens were obtained from the olfactory mucosa at the caudal part of the nasal septum and the ethmo-turbinates bones after necropsy of the animals. It was designated to investigate the olfactory mucosa by using electron microscope and immuno-histochemical technique in order to obtain more information about the cyto-architecture of such mucosa in dogs. The results showed that, the olfactory mucosa was formed of a superficial pseudo-stratified columnar ciliated epithelial layer covered with mucoid surface layer, and deep lamina propria formed from loose connective tissue. The epithelium comprised olfactory, supporting and basal cells in addition to secretory scarcely scattered microvillous cells. The olfactory cell was abundant, and appeared spindle-like, its dendrite had a peculiar bulbous and expanded olfactory knob associated with vigorous number of long olfactory cilia projected into the free epithelial surface. The axonal hillock had distally extended axonal fibers piercing the basal lamina and converged to form large axonal bundles at the lamina propria. The supporting cells appeared to be wedged-like columnar cells with wide apical part impacted with secretory granules and bearing microvilli intertwining with the olfactory cilia, and its distally tapering portion inter-digitated with the lamina propria. The basal cells were irregular cells, and distinguished into horizontal and globose basal cells. Both of the olfactory and supporting cells displayed deviated developmental stages, as well as degenerated apoptotic cells, indicating the cyclic turnover of these cells. As well, these cells had the usual cytoplasmic cell organelles, but the olfactory one had more abundant mitochondria, meanwhile the supporting cells had more endoplasmic reticulum. With regards to the immuno-reaction, the supporting cells had positive immuno-reaction for cytokeratin intermediate filaments and vice versa, in the olfactory one, which lacked cytokeratin. The horizontal basal cells had positive immuno-reaction for cytokeratin, and proposed to be the stem progenitor cells of the supporting cells. Meanwhile, the globose cells had negative immuno-reaction for cytokeratin, so they proposed to be the stem basal progenitor cells of olfactory one. GFAP positive reaction appeared at nerve bundles in the lamina propria, while alpha smooth muscle actin showed strong positive reaction at the wall of blood vessels. The lamina propria composed of loose connective tissue, containing exocrine tubulo-acinar Bowman's glands that contained mixed, mainly neutral muco-polysaccharides and bundles of olfactory axons, in addition to vascular elements.

Keywords: Olfactory, ultrastructure, dogs, histochemistry, immuno-histochemistry.

INTRODUCTION

It was an established fact, that the olfaction is a vital sense in most mammals, as the olfactory system detects and processes chemicals in the environment providing long-range information that is necessary for survival, and many vertebrates rely mainly on olfactory input for social interaction, food locating,

migration, reproduction and alerting to the presence of predators (Morrison and Costanzo, 1992b; and Walker, Hall, Walker, Kendal-Reed, Hood, and Niu, 2003).

The dog has been known as a macrosmatic animal which has an olfactory acuteness for detecting of odorant concentration at level of 1-2 parts per trillion (Smith, Bhatnagar, Tuladhar, and Burrows,

2004; and Walker, Walker, Cavnar, Taylor, Pickel, Hall, and Suarez, 2006).

The dogs have incredible sense of smell, so they are utilized for many purposes like sniffing and detecting of drugs, bombs, duds, (Wells and Hepper, 2003; Hepper and Wells, 2005; and craven, 2008) and recently, cancer melanoma (Pickel, Manucy, Walker, Hall, and Walker, 2004)

From the hitherto found in the previous literatures, the macro- and micro-anatomical features and structure of the dogs' nasal cavity and its lining mucosa have been thoroughly described and published by many authors such as (Getty, 1975; Nickel, Schummer, and Seiferle, 1979; Menco, 1980; Adams and Wiekamp, 1984; Hirai, Kojima, Shimada, Umemura, Sakai, and Itakurat, 1996; Evans and de Lahunta, 2013; Frandson, Wilke, and Fails, 2013; and konig and liebich, 2014). Meanwhile, the literatures concerned with the ultra-structures of the olfactory epithelium in dogs were scanty, so that the present investigation was designated to throw more light on the ultra-structure features as well as to identify the specific cell types constituted the cellular populations of the olfactory epithelium in dogs, using electron microscope, in addition to immuno-histochemistry.

MATERIAL AND METHODS

The present investigation was carried-out on the olfactory mucosa of clinically healthy and mature five dogs of both sexes of native breed (*Canis Familiaris*) ranging from 8-18 months age. The fresh skulls were collected directly after necropsy of these animals, and were submitted for longitudinal sections at

their median line as well as for transverse sections at the fronto-nasal suture.

The tissue specimens of the olfactory mucosa were excised from distinct areas that represented by: the caudal portion of the nasal septum, the frontal sinus, the roof of the nasal fundus and the entire mass of the ethmo-turbinates. The tissue specimens were carefully stripped from the underlying bones by aid of the dissecting microscope; the collected specimens were segregated and submitted for special suitable fixations and processing techniques.

For electron microscopic investigation (scanning and transmission), the tissue were prepared, processed, examined and photographed under a JEOL JEM-2100 TEM and a JEOL JSM 6510 lv SEM according to procedures adopted by Electron Microscopy Unit, Mansoura University.

The tissue slides, which were utilized for immuno-histochemistry were prepared, sectioned at 5 μ m thickness, and mounted by three types of anti-markers antibodies according to (Shi, Guo, Cote, Young, Hawes, Shi, Thu, and Taylor, 1999; Petrosyan, Tamayo, and Joseph, 2002; and Furukawa, Nagaike, and Ozaki, 2017) at Departments of Pathology, Faculty of Medicine of both Mansoura and Tanta University and Pathology Laboratory of OCMU of Mansoura University. The utilized antibodies were tabulated in table (1).

The slides of the previous mentioned technique were examined and photographed under light binocular microscope.

The nomenclatures used during this work were adopted by *Nomina Anatomica Veterinaria* (2012) and *Nomina Histologica Veterinaria* (2018).

RESULTS

A- Electron microscopy findings:

At the level of scanning electron microscopy investigation, the free luminal surface of the olfactory epithelium revealed a huge number of interspaced clutches of intertwining fine filaments representing uprightly oriented cilia and microvilli of the olfactory and supporting cells respectively. Such cilia did not have a wavy-like arrangement of the respiratory cilia (Fig. 1). As well, the main component cells of the olfactory epithelium had become apparently distinguished on basis of its electron texture into; short basal cells with more electron density, long supporting cells with moderate electron density and fusiform olfactory cells with electron translucent profile. Moreover such epithelium revealed interlacing fine membranous filaments (Fig. 2).

At the level of transmission electron microscopy investigation, the main component cell types of the olfactory epithelium became clearly discrete and easily distinguished on basis of their fine ultra-structures into; olfactory, sustentacular and basal cells, in addition to scarcely scattered apical microvillus and apoptotic cells. Such epithelium was rested on a thin delicate basal lamina.

The olfactory cells became clearly evident and each of which was distinguished into; long narrow supra-nuclear dendritic portion, wide perikaryon and narrow short axonal hillock. The dendritic portion appeared to be drum-stick-like that had a long narrow cylindrical rod-like stalk and enlarged dome-like terminal end named the olfactory vesicle or knob (Fig. 3). Such olfactory knob was insinuated in between the supra-nuclear portion of the supporting cells and protruded to nearby or even onto the epithelial surface, where they

had peculiar surface extensions that anchored and partially overlapped or even hidden the free apical surface of the surrounding supporting cells (Fig. 3 & 4).

Numerous olfactory cilia were clearly protruded from almost entire free surface of the olfactory knob in standing and upright direction onto the epithelial surface as they interweaving with the surrounding microvilli of the sustentacular cells. Such cilia were appeared to be extended from the so-called basal bodies or corpuscles, which aligned on the interior face of plasma membrane of each olfactory knob. Each cilium was a hollow long cylindrical filament measured about $8\mu\text{m}$ in its length and $0.44\mu\text{m}$ in its diameter, ended by tapering end, and appeared to have a characteristic structure of non-motile cilia, as each cilium displayed the typical structure and arrangement of nine peripheral doublets and two axial microtubules. Moreover, the exterior surface of each cilium was appeared to be studded by an apparent fine pin granulation point seemed to be sensory receptors (Fig. 3, 5 & 6).

The cytoplasm of the olfactory knob appeared to be had electron lucent texture, displayed the liner oriented pattern of the electron dense ciliary basal bodies underneath the plasma membrane of the free apical surface, and revealed widely distributed rod-like electron dense mitochondria, as well as vesicles of both smooth and rough endoplasmic reticulum. Moreover, the cytoplasm revealed numerous electron lucent and irregularly distributed oval or even rounded vesicles of variable sizes and dimensions ranged from $0.18\text{-}0.94\mu\text{m}$. As well, the dendritic stalk had electron lucent cytoplasm, but had relatively more abundant rough endoplasmic reticulum nearby the nucleus and few mitochondria in relation to the knob (Fig. 5, 6, 7 & 8).

The perikaryon of the neuron was clearly colonized by a large oval or even oblong

nucleus with irregular outline and surrounded by a narrow rim of cytoplasm that contained mitochondria. Such nuclei appeared to be mitotically active and contain two nuclei and dispersed euchromatin (Fig. 3, 4 & 7).

The infra-nuclear axonal hillock was appeared to be short conical or funnel-like that succeeded by an apparent olfactory axonal filament extended in between the basal cells until piercing the basal lamina to gain the lamina propria and contributed into nerve fascicles. The cytoplasm of such portion was electron translucent and had numerous electron dense neuro-filaments and mitochondria (Fig. 3 & 4).

On the other side the olfactory epithelium revealed scarcely scattered opaque apoptotic olfactory cells, which had high electron density associated with over condensation of both nuclear and cytoplasmic organelles together with nuclear deformity (Fig. 4).

The supporting cells were vertically oriented columnar cells that extend the entire thickness of the olfactory epithelium and appeared to be long tapering slender or even wedged or cone-like where they displayed a long wide apical portion succeeded by narrow and tapering one. The wide apical portion lodged the nucleus and appeared to be intercalated with the dendrites of the surrounding olfactory cells, its free surface bearing fine brushy microvilli that intervened with the olfactory cilia. The tapering portions were insinuated together with the axonal filaments in between the basal cells to reach the basal lamina (Fig. 3, 9, 10 & 11).

The sustentacular cells displayed cyclic secretory functional activity, where some of which appeared to be still immature or gain into quiescent resting phase, as it had no secretory granules. Meanwhile, another cells revealed vigorous secretory activity and had abundant secretory granules (Fig. 9, 10 & 11).

In correlation with such secretory activity, the nuclei of such cells became polymorphous, and were pushed nearby the tapering narrow portions. The cytoplasm of the quiet resting cells displayed more electron density and appeared to be rich in cytoplasmic organelles, as they revealed many electron lucent spherical cytoplasmic vesicles of variable size like those observed in the olfactory cells, but they had comparatively dimensioned size, electron dense rod-like mitochondria specially at the tapering part, together with spherical vesicles of smooth and rough endoplasmic reticulum (Fig. 9). On the other hand, the wide apical portions of the functionally active cells were appeared to be fulfilled with closely impacted secretory vesicles containing secretory granules. At the same time, the cytoplasm was represented by a narrow rim with clear rod-like patches of mitochondria. The nucleus appeared to be pushed more distally by the accumulated vigorous secretory end products (Fig. 10 & 11). Also, the narrow tapering part was appeared to be engaged in between the surrounding basal cells, and had basal membranous indentation, which interlocked with the underlying connective tissue lamina propria. Moreover, its cytoplasm was appeared to have electron dense rod-like mitochondria as well as rough and smooth endoplasmic reticulum (Fig. 10 & 11). In addition to the three distinct component cell types of the olfactory epithelium, the present study revealed an apparent additional fourth cell type. Such cells were scarcely scattered at the apical portion of the epithelium, nearly similar to the sustentacular cells, but they were relatively short, and had sparse stubby microvilli and electron lucent cytoplasm with paucity of the cytoplasmic organelles, in contrast to the usual supporting cells, so these cells may be represented a transitional developmental stage of supporting cell (Fig. 9).

The basal cells were located at the lower portion of the olfactory epithelium and rested

on a thin delicate electron translucent basal lamina (Fig. 4). As well, these cells had irregular outline, and displayed interspaces for passage of both, the tapering process of sustentacular cells and the axonal filaments of the olfactory receptor cells during their way to the basal lamina (Fig. 4 & 12). Also, these cells revealed fine inter-membranous cytoplasmic digitations with the surrounding cells. Moreover, these cells displayed more electron density, and each cell appeared to be closely packed by a large voluminous nucleus with narrow rim of cytoplasmic envelope. The nuclei had irregular outlines, and appeared to be polymorphous. Each nucleus contained one or two nucleoli of high electron density and dispersed euchromatin reflecting the high mitotic activity of these cells. The cytoplasmic rim of each cell appeared to be electron dense, and had rod-like mitochondria of high electron density. Furthermore, these basal cells were clearly distinguished into basal horizontal and globose cells. The horizontal basal cell was deeply located to the globose one, and it had an oval outline with its long axis nearly parallel to the basal lamina, meanwhile the globose cell had a globular or even pyramidal outline with its long axis almost vertical on the basal lamina (Fig. 12 & 13).

B- Immunohistochemical findings:

The immunohistochemistry investigation of the olfactory epithelium was utilized by using specific proteins anti-markers in order to identify and approximate the position of the component cells.

The monoclonal Cytokeratin 19 (MCF-7) antibody exhibited positive moderate immune-reaction at the supra-nuclear region of the quiet and resting supporting cells, as well as at the glandular epithelium of the Bowman's glands, but it exhibited more intense reaction at the horizontal basal cells and at the infra-tapering processes of the active secretory supporting cells at the lower portion of the olfactory epithelium as well as at the cytoplasmic rim enclosing the apical secretions. Neither the olfactory cells, nor the globose basal cells had any reaction against cytokeratin antibody (Fig. 14 & 15).

Polyclonal anti GFAP antibody gave positive strong immuno-reaction for inter-fascicular glia fibrils of the nerve fascicles at the lamina propria. Such axon bundles were enveloped by a fibroblastic connective tissue sheath. Otherwise, the olfactory mucosa gave negative non-specific reaction (Fig. 16).

Monoclonal alpha smooth muscle actin antibody gave strong reaction only at the interstitial tissue fibers in-between the glandular acini, around its exocrine duct, and at the walls of the blood vessels. Otherwise, the olfactory mucosa gave negative non-specific reaction (Fig. 17)

Table (1): The anti-markers antibodies have been used in this study:

Primary Antibody	Source	Clone	Host	Company	Dilution Factor
Cytokeratin 19	Human	Monoclonal MCF-7	Mouse	Thermo-Scientific	1:50
GFAP	Human	Polyclonal	Rabbit	Master Diagnostica	1:50
Alpha smooth muscle actin	Human	Monoclonal 1A4	Mouse	DAKO Code:M0851	1:100

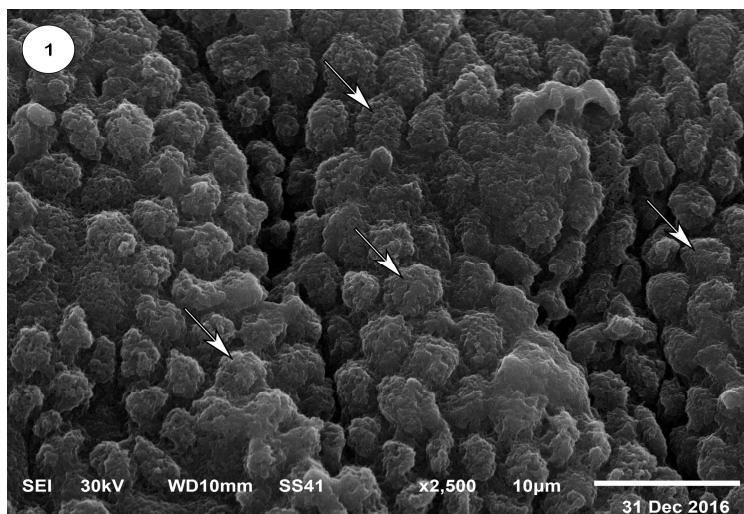


Fig. (1): Scanning electron micrograph of the luminal surface of the olfactory epithelium of a dog at septum nasi showing, inter-spaced clutches of intervening cilia and microvilli (arrow). Bar = 10 µm.

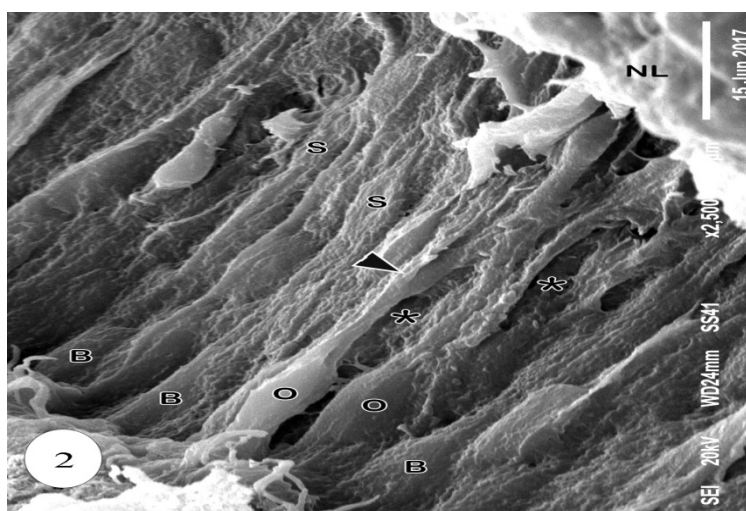


Fig. (2): Scanning electron micrograph of the olfactory epithelium of a dog at septum nasi showing, basal (B), supporting (S) cells with more electron density, and olfactory cells(O) and its narrow dendritic portion (arrow head) with moderate or less electron density. Note: the interlacing fine membranous fibers in-between cells (asterisk), and the nasal lumen (NL). Bar = 10 µm.

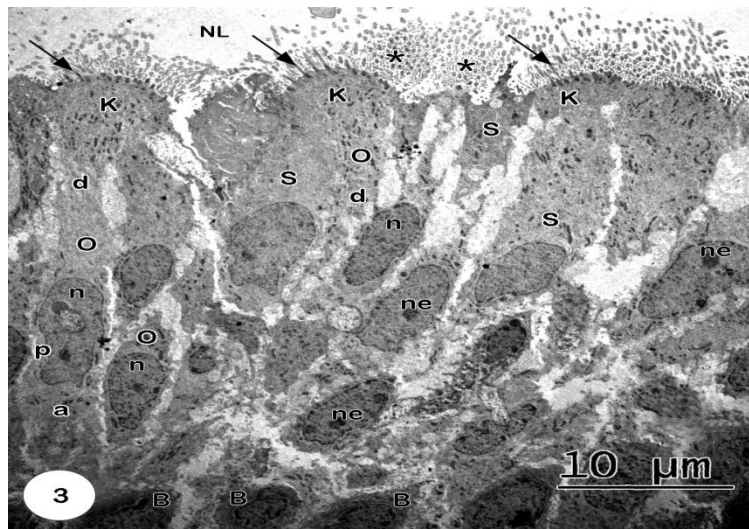


Fig. (3): Transmission electron micrograph of the olfactory epithelium of a dog at ethmo-turbinates showing, electron texture of olfactory (O), supporting (S) and basal (B) cells, perikaryon (p), olfactory knob (k) of supra-nuclear dendrite stalk (d) and infra-nuclear axonal hillocks (a) of olfactory cells, projected cilia (arrow) and microvilli (asterisk) at the nasal lumen (NL). Note: the nuclei (n) and the nucleoli (ne) of the cells. Bar = 10 μm.

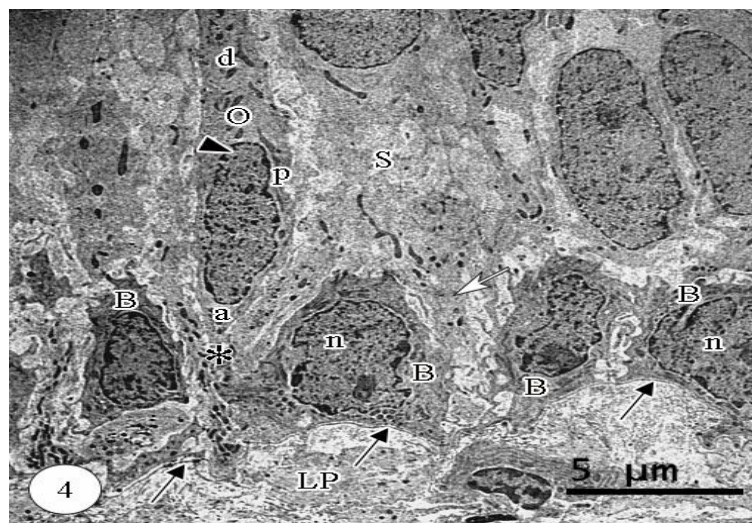


Fig. (4): Transmission electron micrograph of the olfactory epithelium of a dog at septum nasi showing, perikaryon (p) with localized euchromatic oblong oval nucleus (arrow head), supra-nuclear dendrite stalk (d) and infra-nuclear axonal hillocks and filaments (a) of olfactory cells (O), narrow tapering basal process (white arrow) of the supporting cells (S). Note: pathway of both axonal fibers and basal processes (asterisk) in between basal cells, polymorphic basal cells (B) with relative large nuclei (n), encircled with narrow cytoplasmic rim, basal lamina (black arrow), and lamina propria (LP). Bar = 5 μm.

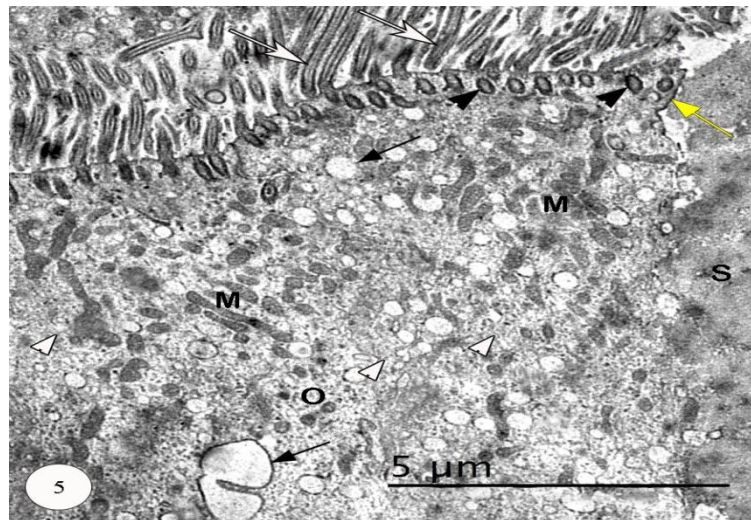


Fig. (5): Transmission electron micrograph of the olfactory epithelium of a dog at septum nasi showing, basal ciliary bodies (black arrow head), cilia (white arrow), electron translucent multiple vesicles (black arrow), electron dense rod-shape mitochondria (M), and electron dense spherical vesicles of smooth and rough endoplasmic reticulum (white arrow head) at the olfactory knob. Note: the complex junctions (yellow arrow) between the olfactory cells (O) and the adjacent supporting cells (S). Bar = 5 μ m.

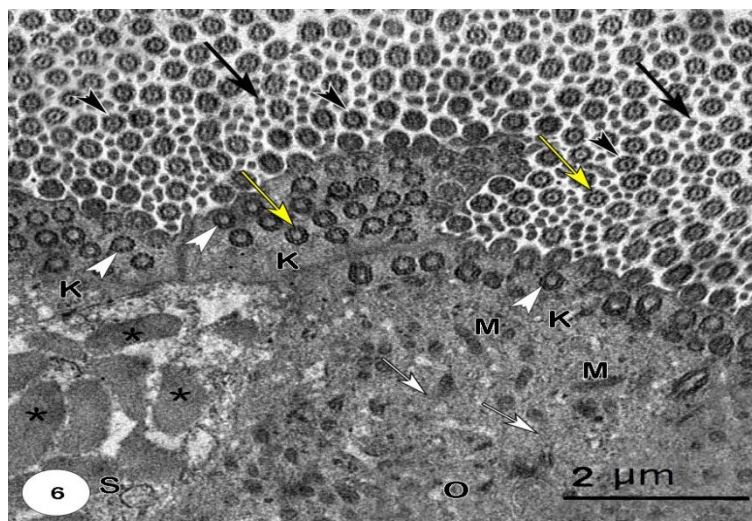


Fig. (6): Transmission electron micrograph of the olfactory epithelium of a dog at ethmo-turbinates showing, expanded free surface of the olfactory knob (k), cross section of both basal bodies (white arrow head) and shafts (black arrow head) of cilia, nine peripheral doublets and two axial microtubules of each cilium (yellow arrow), intervening microvilli (black arrow) in between the cilia, electron dense rod-like mitochondria (M), and electron dense spherical vesicles of smooth and rough endoplasmic reticulum (white arrow) at the olfactory knob. Note: the olfactory cells (O), and the secretory granules (asterisk) at the supra-nuclear portion of the supporting cells (S). Bar = 2 μ m.

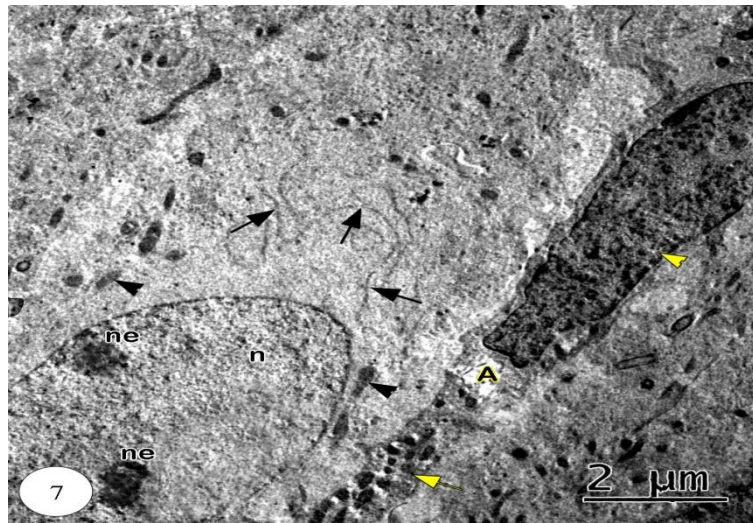


Fig. (7): Transmission electron micrograph of the olfactory epithelium of a dog at septum nasi showing, well organized peri-nuclear rough endoplasmic reticulum (black arrow), darkly stained rod-like mitochondria (black arrow head) at the dendritic stalk, euchromatic nucleus (n) of olfactory cell with two nucleoli (ne). Note: apoptotic olfactory cell (A) with nuclear deformity (yellow arrow head) and cytoplasmic condensation (yellow arrow). Bar = 2 μm.

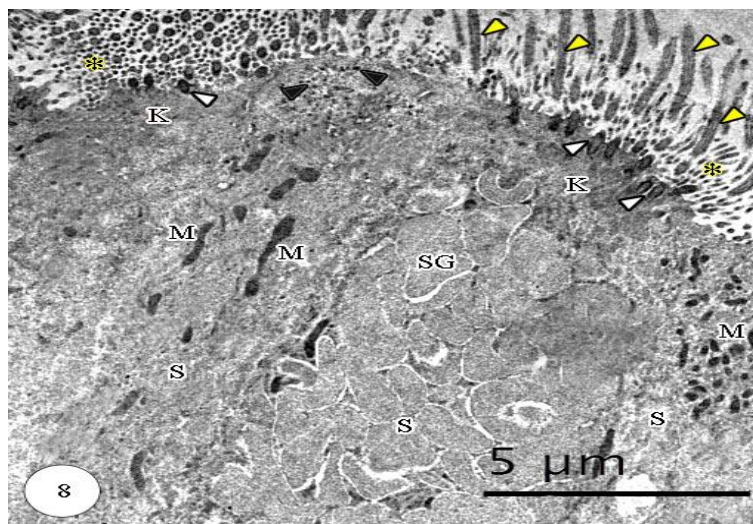


Fig. (8): Transmission electron micrograph of the olfactory epithelium of a dog at ethmo-turbinates showing, overlapped expanded free surface of the olfactory knob (k) over the supporting cells (S), basal bodies (white arrow head) of cilia, microvilli (asterisk) in between the cilia (yellow arrow head), rod-like mitochondria (M) and smooth endoplasmic reticulum (black arrow head), and secretory granules (SG) of supporting cells. Bar = 5 μm.

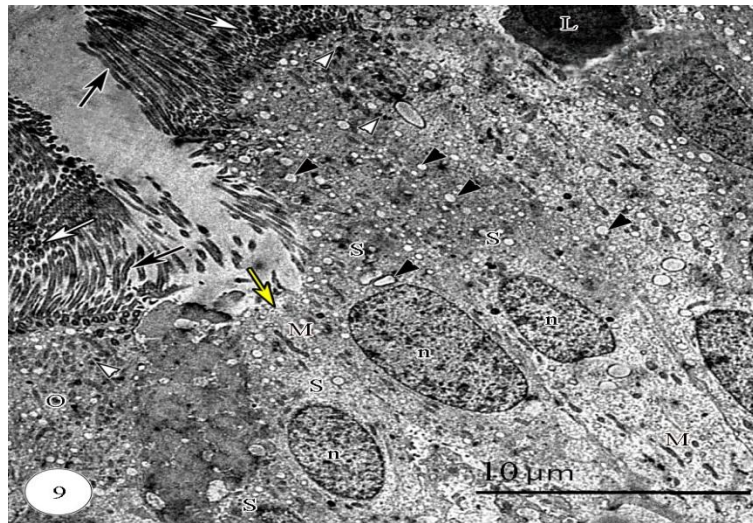


Fig. (9): Transmission electron micrograph of the olfactory epithelium of a dog at ethmo-turbinates showing, electron texture of quiet resting supporting cells (S), multiple electron lucent rounded small vesicles (black arrow head), electron dense rode-like mitochondria (M) and spherical smooth endoplasmic reticulum (white arrow head). Note: the nucleus (n) and the apical villi (white arrow) of supporting cells, apparent microvillous cell (yellow arrow) with its short stubby microvilli, olfactory cells (O) with long cilia (black arrow), and moderate electron dense scarcely scattered intraepithelial lymphocytes (L). Bar = 10 μm.

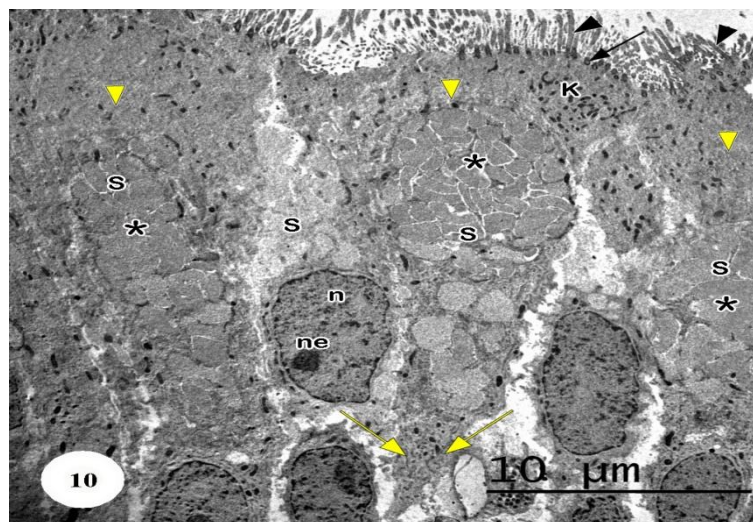


Fig. (10): Transmission electron micrograph of the olfactory epithelium of a dog at ethmo-turbinates showing, wedge-like supporting cells (S) with its apical (yellow arrow head) and foot-like process tapering (yellow arrow) portions, accumulated cytoplasmic secretory end products (asterisk), and its nucleus (n) contained nucleolus (ne). Note: olfactory knob (k), and basal body (black arrow) of projecting olfactory cilia (black arrow head). Bar = 10 μm.

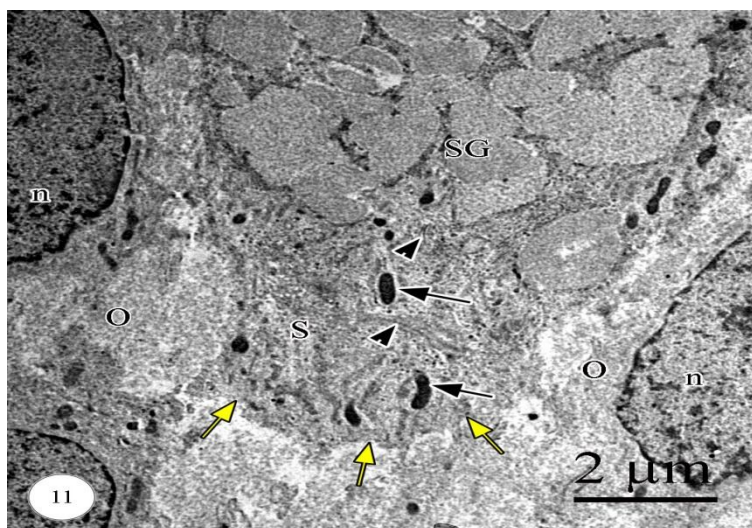


Fig. (11): Transmission electron micrograph of the olfactory epithelium of a dog at septum nasi showing, insinuated narrow tapering part of secretory active supporting cells (yellow arrow) in between adjacent olfactory cells (O) and its distal indentation with lamina propria, electron dense rode-like mitochondria (black arrow), electron lucent rough endoplasmic reticulum (arrow head), and secretory granules (SG) of supporting cells (S). Note: the nucleus (n) of the olfactory cells. Bar = 2 μm.

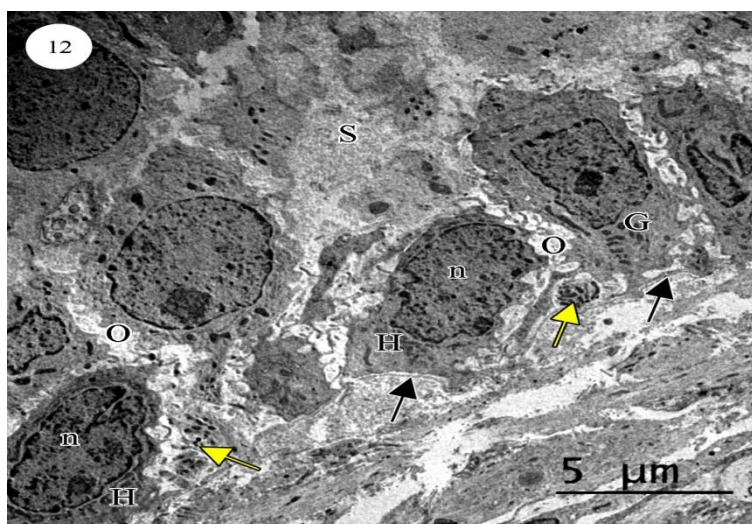


Fig. (12): Transmission electron micrograph of the olfactory epithelium of a dog at ethmo-turbinates showing, globose basal (G) and horizontal basal (H) cells, mitotic nuclei (n) surrounded by narrow cytoplasmic rim. Note: collection of nerve axons (yellow arrow) of olfactory cells (O) at the lower part of epithelium before passing basal lamina (black arrow), and supporting cell (S). Bar = 5 μm.

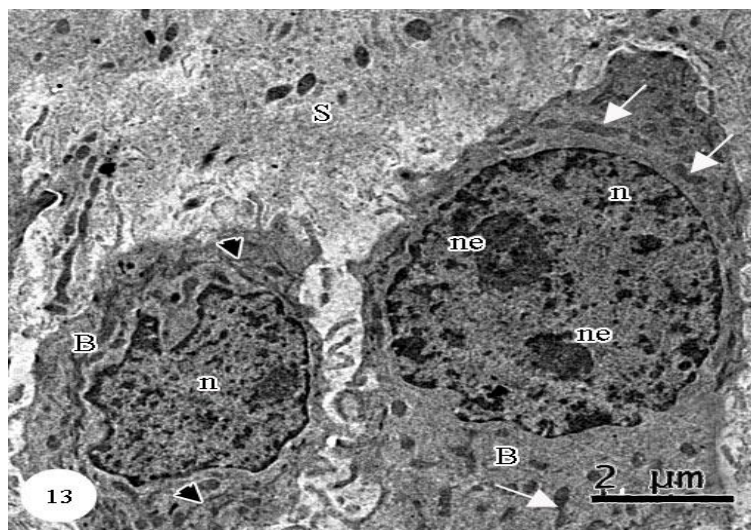


Fig. (13): Transmission electron micrograph of the olfactory epithelium of a dog at ethmo-turbinates showing, voluminous nucleus (n) of basal cells (B) with high mitotic activity, contained two prominent nucleoli (ne), and encircled by narrow cytoplasmic rim that contained electron dense rode-like mitochondria (white arrow) and rough endoplasmic reticulum (arrow head). Note: the supporting cells (S). Bar = 2 μ m.

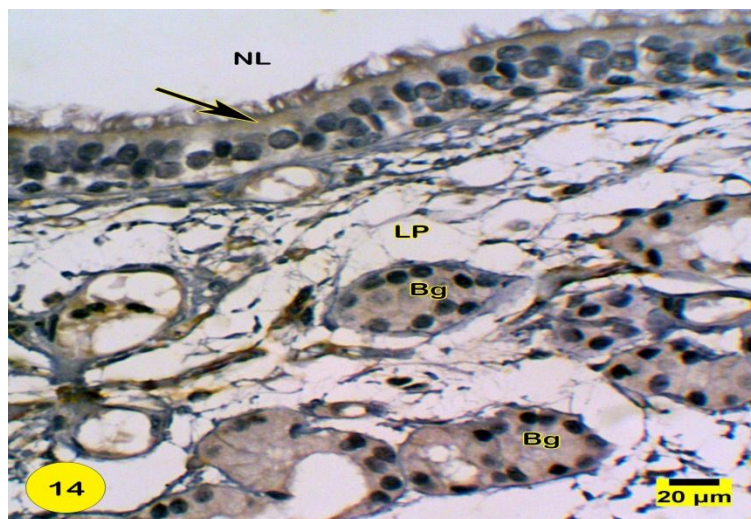


Fig. (14): A Light photomicrograph of the olfactory mucosa of a dog at the septum nasi showing, immuno-reactivity of Monoclonal Cytokeratin 19 (MCF-7) antibody exhibited positive reaction at the supra-nuclear portion of the supporting cells (arrow), and at the glandular epithelium of the Bowman's glands (Bg) at the level of lamina propria (LP). Note: nasal luminal surface of the epithelium (NL). Hematoxylin counter-stain. Bar = 20 μ m.

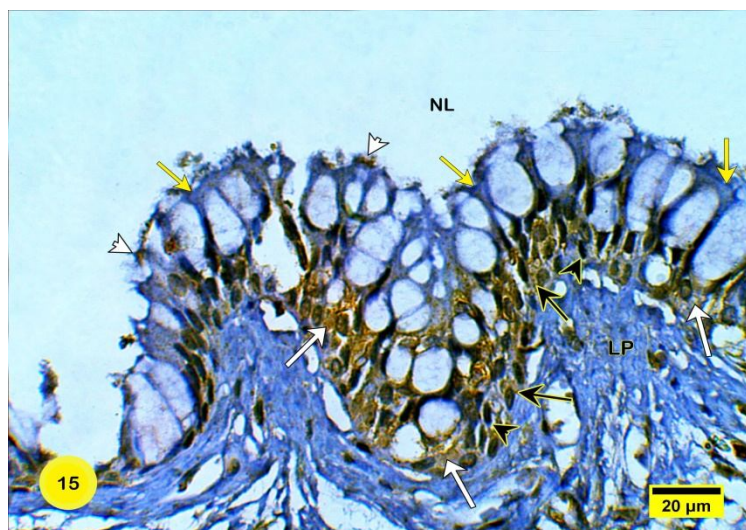


Fig. (15): A Light photomicrograph of the olfactory mucosa of a dog at ethmo-turbinates showing, immuno-reactivity of Monoclonal Cytokeratin 19 (MCF-7) antibody exhibited intense reaction at the horizontal basal cells (black arrow), the tapering process of secretory active supporting cells (white arrow) at the lower part of the epithelium, as well as at the cytoplasmic rim investing the apical secretions (white arrow head). Note: negative immune-reaction at the globose basal cells (black arrow head) and olfactory neurons (yellow arrow), Lamina propria (LP), and nasal lumen (NL). Hematoxylin counter-stain. Bar = 20 μ m.

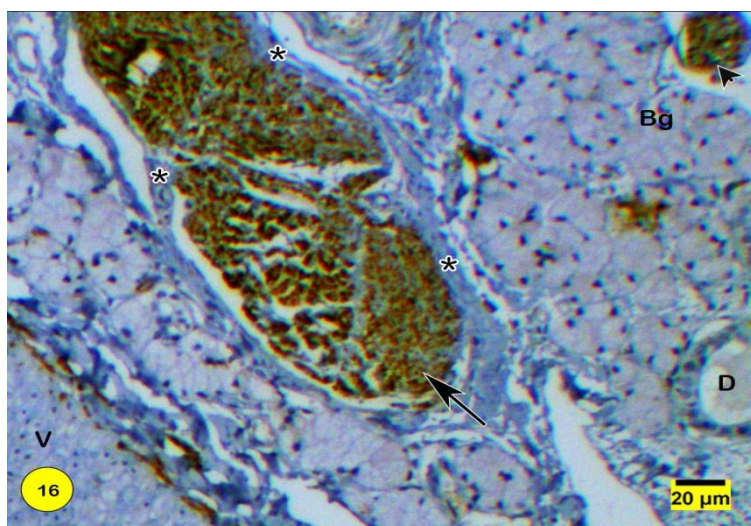


Fig. (16): A Light photomicrograph of the olfactory mucosa of a dog at septum nasi showing, immuno-reactivity of polyclonal GFAP antibody, strong reaction for the inter-fascicular filaments of glia cells (arrow) at the large nerve fascicles that enveloped by a fibroblastic connective tissue sheath (asterisk), and small nerve axons (arrow head). Note: the blood vessels (V) and the ducts (D) of the Bowman's glands acini (Bg). Hematoxylin counter-stain. Bar = 20 μ m.

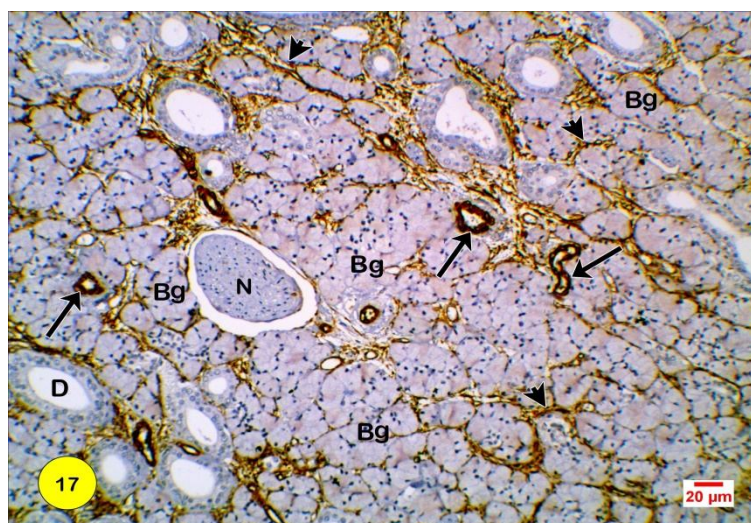


Fig. (17): A Light photomicrograph of the olfactory mucosa of a dog at septum nasi showing, immuno-reactivity of monoclonal alpha smooth muscle actin antibody, intense reaction for the interstitial tissue fibers (arrow head) in-between the glandular acini of the bowman's glands (Bg) and its ducts (D), as well as at the wall of the blood vessels (arrow). Note: negative nerve bundles (N). Hematoxylin counter-stain. Bar = 20 µm.

DISCUSSION

The present study observed that the olfactory mucosa attended yellowish brown coloration in contrast to the bright red coloration of the respiratory mucosa. Such coloration was owing to lipid content in the secretion of the Bowman's glands (**Evans and de Lahunta, 2013**). It covered the caudal part of the nasal septum and ethmo-turbinates at the nasal fundus. Such condition was correlated with that mentioned in other mammals (**Smith, et. al., 2004**). Further, the present observation was correlated with that described by (**Pihstrom, Fortelius, Hemila, Forsman, and Reuter, 2005; and Craven, 2008**) in dog, as who found that the ethmo-turbinates of dog had more complexity and prominent folded lamellae, thereby provided an extensive surface for the olfactory mucosa and its contained neuro-receptors that perhaps predictive morphological indicator for the olfactory capability in dog.

The general cyto-architecture of the olfactory mucosa of dog was closely similar to that reported by (**Ding and Dahl, 2003; and Harkema, Carey, and Wagner, 2006**), where such mucosa was composed of a superficial epithelial layer of pseudo-stratified columnar ciliated epithelium containing olfactory, supporting and basal cells, and covered by a mucus layer, as well as a deeper layer of lamina propria of loose connective tissue. Moreover, the present study revealed an additional microvillar cells similar to that recorded in man (**Moran, Rowley, Jafek, and Lovell, 1982; and Morrison and Costanzo, 1990**) and dog (**Okano, Weber, and Frommes, 1967**).

In agreement with (**Menco and Morrison, 2003; and Evans and de Lahunta, 2013**), the sensory receptors of dog were primary sensory bipolar neurons, which had large perikaryons, apically directed dendrites and basally extended axonal filaments. In dog, the olfactory cells were recognized to be the

most encountered cells of the olfactory epithelium, in association with yielding many axonal fibers pierced the basal lamina and converging information of great axonal bundles at the lamina propria. Such findings gave a predictive excellent odor detection and sensitivity in dogs.

Unlike, the large oval olfactory knob that recorded in **(Menco, Bruch, Dau, and Danho, 1992; and Menco, 1997)**, the olfactory knob of dog had peculiar bulbous dome-like with expanded free surface that gave rise to significantly vigorous and much numbers of protruded long cilia into the epithelial surface. Such findings may permit a direct correlation between the length and number of olfactory cilia, and acute olfactory sensitivity in dog; as such cilia were proved to be the loci of the odor perception. Such interpretations were supported by statement of **(Getchel, Margolis, and Getchell, 1984; and Getchel, Su, and Getchell, 1993)**, as who said that, the odor binding receptors were located within the cilia, so they considered the primary site of initial sensory transduction, where the odorant molecules binding the receptors and create receptor potential signals, as well as by **(Leinders-Zufall, Greer, Shepherd, and Zufall, 1998)** who stated that the cilia were encircled with odorants, sensitive adenyle cyclase and transductory enzymes.

In general with that observed in vertebrates by **(Morrison and Costanzo, 1992a)**, the olfactory cilia of dog were intervening with the microvilli of the sustentacular cells, thereby forming a blanket layer submerged in the surface mucus layer. Each cilium exhibited the typical oriented pattern of the microtubules "9+2" of the motile cilia, in spite of these olfactory cilia belong to Kino-cilia, where non-motility was attributed to the restrictive embedment of the mucus layer.

The present study revealed that some of the olfactory neurons had deviated, unusual spindle-like form of the mature neurons together with polymorphous nuclei, as well some of the supporting cells revealed heterogeneous population of deviated wedged-like form of mature supporting cells. Such observations suggested transitional, intermediate developmental stages of both olfactory and supporting cells during their maturation. Furthermore, the olfactory epithelium revealed apoptotic cells indicating cellular regeneration. Such observations may reflect that, the olfactory epithelium had continuous turnover and the basal cells act as stem progenitors cells for both olfactory and supporting cells.

The fore mentioned observations and postulations have been strengthened and evaluated by **(Schwob, Youngentob, and Mezza, 1995)**, as who said that the induced experimental damage of the olfactory mucosa in mice followed by regeneration and establishment of the normal cellular architecture and the functional activity of such epithelium. As well as, by statement of **(Caggiano, Kauer, and Hunter, 1994; Weiler and Farbman, 1998; and Jang, Youngentob, and Schwob, 2003)**, who recorded that the olfactory epithelium had continuous regeneration probably related to its continuous exposure to noxious environmental agents.

In agreement with **(Morrison and Costanzo, 1992b; and Huard and Schwob, 1995)**, the basal cells at the lower part of the olfactory epithelium revealed continuous mitotic activities, and they were distinguished into horizontal and globose basal cells. Further, both horizontal basal and supporting cells gave intense immuno-reaction for cytokeratin filaments characterized the epithelial cells. Meanwhile, both of globose basal and receptor cells gave negative immuno-reaction for

cytokeratin, indicating lacking of cytokeratin filaments in these cells. Such findings suggested that, the horizontal basal cells were the stem basal cells progenitor for renewing the supporting cells. Meanwhile, the globose ones were the stem basal progenitor cells for renewing the olfactory cells. Such opinion was confirmed in such ways as the present study observed that the supporting cells had ultrastructure tonofilaments, and gave immuno-reaction for cytokeratin, just finding their designation as epithelial cells. Meanwhile, the mature olfactory cells had no intermediate neuro-filaments and gave negative immuno-reaction for cytokeratin, just finding their designation as unique primary neurons. Furthermore, the fore mentioned postulations have been confirmed by (Yamagishi, Hasegawa, Takahashi, Nakano, and Iwanaga, 1989; and Suzuki and Takeda, 1991) who said that, the mature olfactory cell gave negative immuno-reaction when tested with varieties of antibodies specific for neuro-filaments. This negative reaction underlined the exceptional nature of the olfactory cells, as these cells are unique among ordinary neurons, as they lacked intermediate neuro-filaments, and they are not permanent, but continuously turned over.

In agreement with (Okano, et. al., 1967), the secretory active supporting cell of the dog had wedged-like form, its web bearing a brushy microvilli intertwining with olfactory cilia, its apical wide part were impacted by positive AB secretion, and its terminal process had foot-like processes inter-digitated with underlying basal lamina and lamina propria. Furthermore, these cells formed many functions as glia-like within the neuro-epithelium (Morrison and Costanzo, 1992b), secretion of acidic mucopolysaccharides, as such secretion maintained the ionic composition of the mucus layer, and aid in oxidation of inhaled toxic agents.

In ultrastructure investigation, both of the olfactory and supporting cells had prominent cytoplasmic organelles, but the supporting cells revealed more abundant both rough and smooth endoplasmic reticulum owing to its secretory nature, and had cytoskeletal tonofilaments. Meanwhile, the olfactory cell lacked the intermediate cytokeratin filaments, and had more abundant mitochondria owing to its significance in metabolism and oxidation of these continuously active cells. As well as, the present study revealed interlacing fine membranous that provide intimate contact between the adjacent cells in agreement with (Rafols and Getchell, 1983).

In agreement with (Vollrath, Altmannsberger, Weber, and Osborn, 1985; and Lee, Park, Bang, Ahn, Moon, Kim, and Shin, 2016), the Bowman's glands were located at the lamina propria and belonged to the tubulo-acinar exocrine and serous glands that pouring their secretion onto the epithelium surface via intra-epithelial ducts.

The present study revealed that, both the supporting cells and the Bowman's glands were constitute the secretory units of the olfactory mucosa, and their secretion were contributes to the surface mucus layer.

The present study observed that, the intra-fascicular fibers encircled the axonal fibers with the large nerve bundles gave positive GFAP immuno-reaction, indicating presence of astrocytes (Schwann glia cells of peripheral axons), As well as wide distribution of minutes, often large blood vessels nearby the large axonal bundles, and appeared positively reacted with alpha smooth muscle actin antibody. Such relation may serve to facilitate the delivery of the nutrient and oxygen to the deeply positioned olfactory ensheathing glia cells.

REFERENCES

- Adams, D. R., and Wiekamp, M. D. (1984):** The canine vomero-nasal organ, *J. Anat.* 138, pp. 771-788.
- Caggiano, M., Kauer, J. S., and Hunter, D. D. (1994):** Globose basal cells are neuronal progenitors in the olfactory epithelium: A lineage analysis using a replication-incompetent retrovirus. *Neuron* 13, pp. 339-52.
- Craven, B. A. (2008):** A fundamental study of the anatomy, aerodynamics, and transport phenomena of canine olfaction. Ph. D. thesis, Mechanical Engineering, The Pennsylvania State University.
- Ding, X. A., and Dahl, A. R. (2003):** Olfactory mucosa: Composition, enzymatic localization, and metabolism. In *Handbook of Olfaction and Gustation* (R. L. Doty, ed.), Marcel Dekker, Inc., New York, pp. 51-73.
- Evans, H. E., and Alexander de Lahunta. (2013):** "*Miller's anatomy of the dog*". 4th edition, Saunders, Elsevier, Chap. 4, Chap. 8, pp. 86, and pp. 340-344 respectively.
- Frandsen, R. D., Wilke, W. L., and Fails, A. D. (2013):** *Anatomy and Physiology of Farm Animals*. 7th edition, Wiley-BlackWell, Chap. 11, pp. 191-192.
- Furukawa, S., Nagaike, M., and Ozaki, K. (2017):** Databases for technical aspects of immunohistochemistry. *J. Toxicol Pathol.* 30, pp. 79-107.
- Getchell, T. V., Margolis, F. L., and Getchell, M. L. (1984):** Peri-receptor and Receptor Events in Vertebrate Olfaction. *Progress in Neurobiology* 23(4), pp. 317-322.
- Getchell, T. V., Su, Z. Y., and Getchell, M. L. (1993):** Mucous Domains – Microchemical Heterogeneity in the Mucociliary Complex of the Olfactory Epithelium. *Ciba Foundation Symposia* 179, pp. 27-50.
- Getty, R. (1975):** Sisson and Grossman's. *The anatomy of the domestic animals*. 5th edition, Volume 2, W. B. Saunders Company, Philadelphia, London, Toronto, Mexico City, Rio de Janeiro, Sydney, Tokyo, Chap. 52, pp. 1560-1562.
- Harkema, J. R., Carey, S. A., and Wagner, J. G. (2006):** The nose revisited: A brief review of the comparative structure, function, and toxicologic pathology of the nasal epithelium. *Vol. 34, No. 3*, pp. 255-258.
- Hepper, P. G., and Wells, D. L. (2005):** How many footsteps do dogs need to determine the direction of an odor trail?. *Chemical Senses* 30, pp. 291-298.
- Hirai, T., Kojima, S., Shimada, A., Umemura, T., Sakai, M., and Itakurat, C. (1996):** Age-related changes in the olfactory system of dogs. *Neuropathology and Applied Neurobiology* 22, pp. 531-539.
- Huard, J. M., and Schwob, J. E. (1995):** Cell cycle of globose basal cells in rat olfactory epithelium. *Dev Dyn* 203, pp. 17-26.
- Jang, W., Youngentob, S. L., and Schwob, J. E. (2003):** Globose basal cells are required for reconstitution of olfactory epithelium after methyl bromide lesion. *J Comp Neurol* 460, pp. 123-40.
- Konig, H. E., and Liebich, H. G. (2014):** The respiratory system, "Veterinary Anatomy of Domestic Mammals". 6th

- edition, Schattauer, chapter 8, pp. 343-349.
- Lee, K. H., Park, C., Bang, H., Ahn, M., Moon, C., Kim, S., and Shin, T. (2016):** Histo-chemical study of the olfactory mucosae of the horse. *Acta Histochemica* 118, pp. 361-368.
- Leinders-Zufall, T., Greer, C. A., Shepherd, G. M., and Zufall, F. (1998):** Imaging Odor-Induced Calcium Transients in Single Olfactory Cilia: Specificity of Activation and Role in Transduction. *Journal of Neuroscience* 18(15), pp. 5630-5639.
- Menco, B. P. M. (1980):** Qualitative and Quantitative Freeze-Fracture Studies on Olfactory and Nasal Respiratory Structures of Frog, Ox, Rat, and Dog .1. A General Survey. *Cell and Tissue Research* 207(2), pp. 183-209.
- Menco, B. P. M. (1997):** Ultra-structural Aspects of Olfactory Signaling. *Chem. Senses* 22(3), pp. 295-311.
- Menco, B. P. M., and Morrison, E. E. (2003):** Morphology of the Mammalian Olfactory Epithelium: Form, Fine Structure, Function, and Pathology. In "*Handbook of Olfaction and Gustation*" (R. L. Doty, ed.), edition 2, Marcel Dekker, Inc., New York, Chap. 2, pp. 17-96.
- Menco, B. P. M., Bruch, R. C., Dau, B., and Danho, W. (1992):** Ultrastructural Localization of Olfactory Transduction Components: The G-Protein Subunit Golf-Alpha and Type-III Adenylyl Cyclase. *Neuron* 8(3), pp. 441-453.
- Moran, D. T., Rowley, J. E., Jafek, B. W., and Lovell, M. A. (1982):** The fine structure of the olfactory mucosa in man. *J. Neurocytol.* 11, pp. 721-746.
- Morrison, E. E., and Costanzo, R. M. (1990):** Morphology of the human olfactory epithelium. *J. Compo Neurol.* 297, pp. 1-14.
- Morrison, E. E., and Costanzo, R. M. (1992a):** Morphology of Olfactory Epithelium in Humans and Other Vertebrates. *Microscopy Research and Technique* 23(1), pp. 49-61.
- Morrison, E. E., and Costanzo, R. M. (1992b):** "Morphology and Plasticity of the Vertebrate Olfactory Epithelium". In *Science of Olfaction*, Chap. 2, pp. 31-50.
- Nickel, R., Schummer, A., and Seiferle, A. (1979):** The respiratory system, "The viscera of the domestic mammals". 2nd ed., Springer-Verlag, Berlin, Heidelberg GmbH, pp. 211-223.
- Nomina Anatomica Veterinarai (2012):** Prepared by the International Committee on Veterinary Gross Anatomical Nomenclature (I.C.V.G.A.N.), 6th edition, the Editorial Committee, Hannover (Germany), Columbia, MO (U.S.A.), Ghent (Belgium), Sapporo (Japan).
- Nomina Histologica Veterinarai (2018):** Prepared by the International Committee on Veterinary Histological Nomenclature (I.C.V.H.N.), 1st edition, the Editorial Committee, Hannover (Germany).
- Okano, M., Weber, A. F., and Frommes, S. P. (1967):** Electron microscopic studies of the distal border of the canine olfactory epithelium. *J. Ultrastruct. Res.* 17, pp. 487-502.
- Petrosyan, K., Tamayo, R., and Joseph, D. (2002):** Sensitivity of a novel biotin-free detection reagent (power vision+) for immunohistochemistry. *J.*

- Histotechnology, Volume 25, pp. 247-250.
- Pickel, D., Manucy, G. P., Walker, D. B., Hall, S. B., and Walker, J. C. (2004):** Evidence for canine olfactory detection of melanoma. *Applied Animal Behaviour Science* 89(1), PP. 107-116.
- Pihstrom, H., Fortelius, M., Hemila, S., Forsman, R., and Reuter, T. (2005):** Scaling of Mammalian Ethmoid Bones Can Predict Olfactory Organ Size and Performance. *Proceedings of the Royal Society B-Biological Sciences* 272(1566), pp. 957-962.
- Rafols, J. A., and Getchell, T. V. (1983):** Morphological relations between the receptor neurons, sustentacular cells and Schwann cells in the olfactory mucosa of the salamander. *Anat. Rec.* 206, pp. 87 -101.
- Schwob, J. E., Youngentob, S. L., and Mezza, R. C. (1995):** Reconstitution of the rat olfactory epithelium after methyl bromide-induced lesion. *J Comp Neurol* 359, pp. 15-37.
- Shi, S. R., Guo, J., Cote, R. J., Young, L., Hawes, D., Shi, Y., Thu, S., and Taylor, C. R. (1999):** Applied immunohistochemistry and molecular morphology. Volume 7, pp. 201-208.
- Smith, T. D., Bhatnagar, K. P., Tuladhar, P., and Burrows, A. M. (2004):** Distribution of Olfactory Epithelium in the Primate Nasal Cavity: Are Microsmia and Macrosmia Valid Morphological Concepts?. *Anatomical Record Part A-Discoveries in Molecular Cellular and Evolutionary Biology* 281 A (1), pp. 1173-1181.
- Suzuki, Y., and Takeda, M. (1991):** Keratins in the developing olfactory epithelia. *Developmental Brain Research* 59, pp. 171-178.
- Vollrath, M., Altmannsberger, M., Weber, K., and Osborn, M. (1985):** An ultrastructural and immunohistological study of the rat olfactory epithelium: Unique properties of olfactory sensory cells. *Differentiation* 29, pp. 243-253.
- Walker, D. B., Walker, J. C., Cavnar, P. J., Taylor, J. L., Pickel, D. H., Hall, S. B., and Suarez, J. C. (2006):** Naturalistic Quantification of Canine Olfactory Sensitivity. *Applied Animal Behaviour Science* 97(2-4), pp. 241-254.
- Walker, J. C., Hall, S. B., Walker, D. B., Kendal-Reed, M. S., Hood, A. F., and Niu, X. F. (2003):** Human Odor Detectability: New Methodology Used to Determine Threshold and Variation. *Chem. Senses* 28(9), pp. 817-826.
- Weiler, E., and Farbman, A. I. (1998):** Supporting cell proliferation in the olfactory epithelium decreases postnatally. *Glia* 22, pp. 315-28.
- Wells, D. L., and Hepper, P. G. (2003):** Directional tracking in the domestic dog, *Canis familiaris*. *Applied Animal Behavior Science* 84, pp. 297-305.
- Yamagishi, M., Hasegawa, S., Takahashi, S., Nakano, Y., and Iwanaga, T. (1989):** Immunohistochemical analysis of the olfactory mucosa by use of antibodies to brain proteins and cytokeratin. *Ann Otol Rhinol Laryngol* 98, pp. 384-388.

الملخص العربي

التركيب الدقيق لمنطقة الشم في الكلاب

صلاح المرسي^١، جلال يوسف^٢، صفوت عبادة^٣، سهر إبراهيم^٤*

قسم التشريح والأجنة، كلية الطب البيطري، جامعة المنصورة

لقد تم إجراء هذه الدراسة على خمسة كلاب سليمة ظاهريا وبالغة في العمر من كلا الجنسين. وقد تم تجميع الانسجة من الغشاء المخاطي الشمي الموجود على الجزء الخلفي من الحاجز الانفي وعظام القرائن الغربالية بعد وفاة الحيوانات مباشرة. ولقد اجريت هذه الدراسة لفحص الغشاء المخاطي الشمي باستخدام الميكروسكوب الالكتروني وفحص كيمياء الخلايا باستخدام أجسام مضادة للبروتينات الموجودة داخل خلايا النسيج، وأيضا للحصول على معلومات أكثر عن التكوين الخلوي لهذا الغشاء في الكلاب، والتي تمتلك حاسة شم قوية ووميزة بين الحيوانات المستأنسة. من خلال هذه الدراسة تم ملاحظة أن النسيج الشمي يتكون من طبقة سطحية عبارة عن ظهارة عمودية طويلة كاذبة التطبق ذات شعيرات شممية على هيئة أهداب حسية ناحية السطح الحر، والتي تغطي بطبقة مخاط سطحية، كما أنه يتكون من طبقة اساسية عميقة تحت مخاطية، وهي عبارة عن نسيج ضام ليفي. تتكون الطبقة الظهارية من ثلاثة أنواع من الخلايا؛ خلايا شممية، داعمة، وخلايا قاعدية، بالإضافة إلى خلايا دقيقة زغبية متناثرة بقلّة بين الخلايا الداعمة. إن الخلية الشممية هي أكثر أنواع الخلايا عددا وتظهر مغزلية الشكل، حيث أن لها تغصنات تمتد وتنتهي بانتفاخ مميز يسمى الحويصلة الشممية، والتي يخرج منها عدد كبير من الشعيرات الشممية الطويلة على السطح الحر للظهارة، بينما القطب المحوري لهذه الخلايا يمتد إلى الاسفل كألياف غير نخاعية عابرة الصفيحة الاساسية إلى الطبقة تحت المخاطية لتتجمع وتكون فيها حزم عصبية كبيرة والتي تعنى العصب الشمي الذي ينتهي في البصلة الشممية بالمخ.

هناك الخلايا الداعمة كاملة النمو التي تظهر كخلايا عمودية طويلة مخروطية الشكل، حيث أن الجزء العلوي من هذه الخلايا يكون واسع وممتلئ بحبيبات مفرزة، ويحمل سطحه الحر خميلات متداخلة مع الشعيرات الشممية، بينما الجزء القاعدي من الخلايا يكون رفيع ودبيب وينتهي بنهايات متشعبة التي تصل إلى الطبقة تحت الشممية. أما بالنسبة إلى الخلايا القاعدية فهي عبارة عن خلايا غير منظمة في الشكل ويمكن تمييزها إلى نوعين من حيث الشكل: خلايا أفقية على الصفيحة الاساسية، والاخرى بيضاوية على عمودية على الصفيحة الاساسية.

يمر كلا من الخلايا الشمية والداعمة بمراحل نمو كما أنه يوجد أيضا خلايا متحللة وذات موت مبرمج، وهذا يدل على التجدد الدورى لهذه الخلايا. كما أن هذه الخلايا تحتوى على عضيات السيتوبلازم المعتادة داخل الخلايا، ولكن الخلية الشمية تحتوى أكثر على الميتوكوندريا (الحبيبات الخيطية)، بينما الخلايا الداعمة تحتوى أكثر على الشبكات الاندوبلازمية. أيضا تظهر الخلايا الداعمة متفاعلة إيجابيا مع الاجسام المضادة للشعيرات التوسطية لبروتين القيراتين الخلوى، على العكس من الخلايا الشمية التى تفتقر إلى القيراتين. تتفاعل الخلايا القاعدية الأفقية أيضا إيجابيا مع الاجسام المضادة للقيراتيت الخلوى، ويرجح أنها تعمل كخلايا جزعية مولدة للخلايا الداعمة من ناحية أخرى، تتفاعل الخلايا القاعدية البيضاوية سلبيا مع الاجسام المضادة للقيراتين، لذلك يرجح أنها الخلايا الجزعية القاعدية المولدة للخلايا الشمية. تتكون الطبقة الاساسية تحت المخاطية من نسيج ضام ليفى يحتوى على "غدد بومان" وهى غدد أنبوبية سنخية ذات إفراز مختلط، ولكن الغالبية تكون للافرازات المتعادلة المكونة من كلا من مخاط + بوليساكيريد، كما أنها تحتوى على حزم عصبية من محاور الخلايا الشمية، بالإضافة إلى أوعية دموية ولمفية. ولقد تم مناقشة النتائج المحصل عليها مع مثيلتها فى الابحاث السابقة.